Consistent Comparison of Drift-Diffusion and Hydro-Dynamic Device Simulations

T. Grasser, H. Kosina, and S. Selberherr

Institute for Microelectronics, TU Vienna
Gusshausstr. 27–29, A-1040 Vienna, Austria

Abstract

Due to the ongoing downscaling of devices non-local effects become more and more important. These non-local effects can be considered in a device simulator using a hydrodynamic (HD) transport model. However, solving the equation system resulting from a HD transport model is known to be much more expensive in computational terms compared to the simpler drift-diffusion (DD) transport model. Thus the HD model should only be used when really necessary in order not to waste valuable computational resources. However, the validity of the DD model must be carefully investigated which is subject to this paper.

1. Introduction

The necessity for the HD transport model is normally checked by comparison of simulation results for DD and HD simulations. Despite the obvious fact that depending on the equation set different principal physical effects are taken into account, the influence on the models for the physical parameters is more subtle. The main reason for this is that in the case of the HD model, information about the average carrier energy is available in form of the carrier temperature. Many physical parameters depend on this average carrier energy, e.g., the mobilities and the energy relaxation times. In the case of the DD model the carrier temperatures are assumed to be in equilibrium with the lattice temperature, that is $T_C = T_L$, hence, all energy dependent parameters have to be modeled in a different way. The carrier energies are estimated using the local energy balance equations which give expressions for the carrier temperatures as a function of the local electric field. These expressions, however, are only valid under homogeneous conditions. Models for the physical parameters for the DD and HD case will be called consistent when they deliver equal results under these homogeneous conditions as will be shown.

2. High-Field Mobility

In the homogeneous situation the electric field and the carrier temperature is related by the local energy balance equation. The two parameters, mobility (μ_ν) and energy relaxation time ($\tau_{\epsilon,\nu}$) have to be modeled properly to guarantee consistency between the DD and the HD model. The following discussion will assume a high-field mobility $\mu_\nu^{\mathrm{LISF}}(E)$ of the form

$$\mu_\nu^{\mathrm{LISF}}(E) \doteq \frac{\mu_\nu^{\mathrm{LIS}}}{\xi + \left((1-\xi)^{\beta_\nu} + \left(\dfrac{\mu_\nu^{\mathrm{LIS}} \cdot E}{v_\nu^{\mathrm{sat}}} \right)^{\beta_\nu} \right)^{1/\beta_\nu}} \tag{1}$$

with μ_ν^{LIS} being the low-field mobility for the carrier type ν. With $\xi = 0$ one obtains the expression published by Caughey and Thomas [1], and with $\xi = 1/2$ the expression used by e.g., Hänsch and Miura-Mattausch [2]. In the following $\tau_{\epsilon,\nu}$ is assumed to be independent of the carrier energy which is valid for large carrier energies. Generalizing the approach proposed in [2] an expression for the HD mobility can be derived starting from the local energy balance equation

$$E^2 \cdot \mu_\nu^{\text{LISF}} = \frac{3 \cdot \text{k}_\text{B} \cdot \Delta T_\nu}{2 \cdot \text{q} \cdot \tau_{\epsilon,\nu}} \tag{2}$$

which must be solved for $E(T_\nu)$, which is then inserted into (1). Unfortunately (2) cannot be explicitly solved in general. However, it can be solved for the most important cases $\xi = 0$ with arbitrary β_ν and for $\xi = 1/2$ with $\beta_\nu = 1$ or $\beta_\nu = 2$. After some algebra one obtains

$$\xi = 0 \quad : \quad \mu_\nu^{\text{LIST}}(T_\nu) = \frac{2^{1/\beta_\nu} \cdot \mu_\nu^{\text{LIS}}}{\left(2 + a_\nu^{\beta_\nu} + \sqrt{a_\nu^{\beta_\nu} \cdot \left(4 + a_\nu^{\beta_\nu}\right)}\right)^{1/\beta_\nu}} \tag{3}$$

$$\xi = \frac{1}{2}, \ \beta_\nu = 1 \quad : \quad \mu_\nu^{\text{LIST}}(T_\nu) = \frac{2 \cdot \mu_\nu^{\text{LIS}}}{2 + a_\nu + \sqrt{a_\nu \cdot (4 + a_\nu)}} \tag{4}$$

$$\xi = \frac{1}{2}, \ \beta_\nu = 2 \quad : \quad \mu_\nu^{\text{LIST}}(T_\nu) = \frac{\mu_\nu^{\text{LIS}}}{1 + a_\nu} \quad \text{with} \quad a_\nu = \alpha_\nu \cdot \Delta T_\nu \tag{5}$$

(5) is the familiar expression used in [2], whereas (3) and (4) are new expressions which must be used for the other values of ξ and β_ν. It should be pointed out that a different approach has been published in [3].

3. Low-Field Mobility

Another important issue when comparing DD and HD simulations is that in conventional mobility models the same low-field μ_ν^{LIS} mobility is used for both transport models. This is problematic for position-dependent local models as is the case with the MINIMOS 6 mobility model [4]. Comparing the diffusion component of the DD and HD current it becomes obvious that the gradient of the carrier temperature causes a different component of the diffusion current. Furthermore, the diffusion current due to the carrier concentration gradient is enhanced by a factor T_ν/T_L. Both effects tend to broaden the carrier distributions in space. This effect is best illustrated in the channel of an NMOS transistor. Since there are less carriers at the surface, the surface mobility model has a different impact on the resulting current which will be larger in the HD case. The surface mobility is modeled by a function which provides a smooth transition between the surface and bulk area using a reference distance as a parameter. To account for the different carrier distributions this reference distance y^{ref} is modified to yield

$$y^{\text{ref,HD}} = y^{\text{ref,DD}} \cdot \left(\frac{T_\nu}{T_L}\right)^\eta \tag{6}$$

These broadened carrier distributions are the reason why the DD model tends to overestimate the electric field as the carrier concentration increases the space charge density in the channel.

4. Examples

The above models were implemented in MINIMOS-NT [5] and several simulations were carried out to confirm the theoretical results and the validity of the simplifying assumptions. As a first example homogeneously doped silicon blocks with sidelength $a = 10$ μm were investigated. Up to medium electric fields the DD and HD currents agree as one would expect. However, for high-fields close to the breakdown voltage the difference was found to be 10%. This arises from the equilibrium contact condition for the carrier temperatures $(T_\nu |_{\text{contact}} = T_L)$ which dramatically violates the local energy balance equation by causing a strong gradient in the carrier temperature. By rearranging (2) a contact model can be derived which eliminates this discrepancy. The resulting electric fields for both contact models are shown in Fig. 1. The I-V curves for n-doped and p-doped semiconductors are shown in Fig. 2. In addition to the matching mobility models, the p-doped semiconductor was simulated using (1) with $\xi = 1/2$ and $\beta_p = 1$ in combination with (5) which is one of the most common errors. As can be seen, the error is intolerably large.

As a second example a long-channel $(L_G = 2.0$ μm) and a short-channel $(L_G = 0.2$ μm) NMOS transistor were considered. For the long-channel device non-local effects were expected to play a minor role. For the HD transport model, simulations with $\eta = 0$ (uncorrected surface distance model) and $\eta = 1$ (corrected surface distance model) were carried out. A comparison of the output characteristics for both transport models is shown in Fig. 3 and Fig. 4. As expected, the device with $L_G = 0.2$ μm shows typical short-channel behavior and $I_D \cdot L_G/W$ is reduced by 50%. Due to velocity overshoot in the channel, the HD currents are considerably higher.

For the final example long- and short-channel PMOS transistors were derived from the NMOS transistors by exchanging N_D with N_A. As the hole mobility is about 1/3 lower compared to the electron mobility the carrier temperatures do not rise to such high levels as compared to the NMOS. Hence, non-local effects do not play such an important role. This is confirmed by the simulated output characteristics which are shown in Fig. 5 and Fig. 6 for both devices. As for the homogeneously p-doped semiconductor both devices were simulated using (1) with $\beta_p = 1$ in combination with (5). As can be seen in Fig. 5 and Fig. 6, the error is again intolerably large.

5. Conclusion

We derived expressions for the HD high-field mobility which are consistent to the familiar expressions used for the DD transport model. Furthermore we modified the heuristic expression for the surface mobility to account for the broadening of the carrier distributions typical to the HD transport model. Finally we demonstrated the importance of these considerations with several simulations.

References

[1] D. Caughey and R. Thomas, "Carrier Mobilities in Silicon Empirically Related to Doping and Field," *Proc.IEEE*, vol. 52, pp. 2192–2193, 1967.

[2] W. Hänsch and M. Miura-Mattausch, "The Hot-Electron Problem in Small Semiconductor Devices," *J.Appl.Phys.*, vol. 60, no. 2, pp. 650–656, 1986.

[3] G. Baccarani and M. Wordeman, "An Investigation of Steady-State Velocity Overshoot in Silicon," *Solid-State Electron.*, vol. 28, no. 4, pp. 407–416, 1985.

[4] S. Selberherr, W. Hänsch, M. Seavey, and J. Slotboom, "The Evolution of the MINIMOS Mobility Model," *Solid-State Electron.*, vol. 33, no. 11, pp. 1425–1436, 1990.

[5] T. Grasser, V. Palankovski, G. Schrom, and S. Selberherr, "Hydrodynamic Mixed-Mode Simulation," in *Simulation of Semiconductor Processes and Devices* (K. D. Meyer and S. Biesemans, eds.), pp. 247–250, Wien, New York: Springer, 1998.
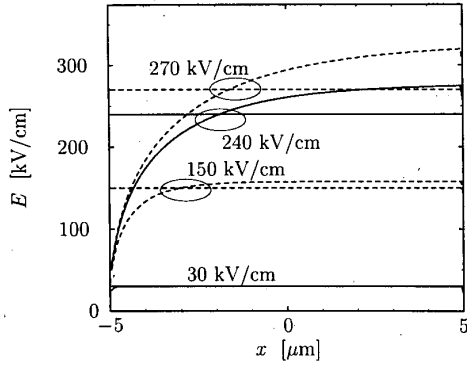
Figure 1: Influence of the boundary condition for the carrier temperatures on the distribution of the electric field inside the homogeneous p-resistor for various bias conditions. The horizontal lines belong to the local equilibrium boundary condition.
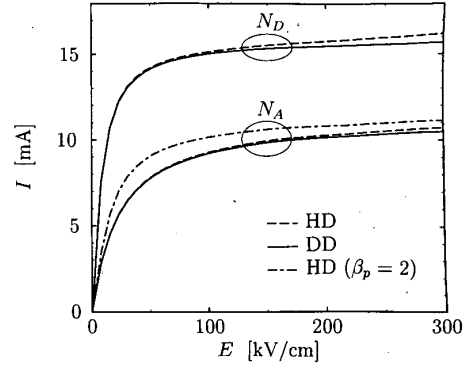

Figure 2: I-V curves for the homogeneously n- and p-doped resistors for DD and HD simulations. In addition, for the p-doped resistor the current for $\beta_\nu = 2$ is shown.
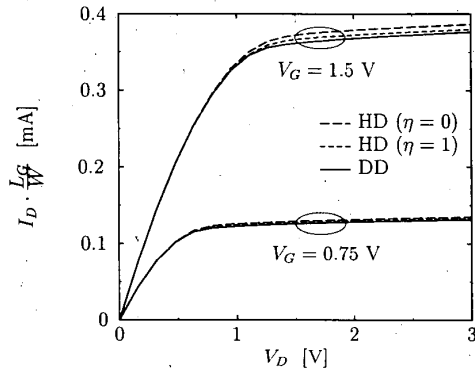

Figure 3: Comparison of the output characteristics of the long-channel NMOS for both transport models.
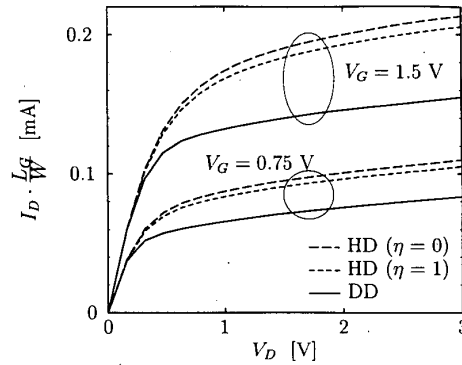

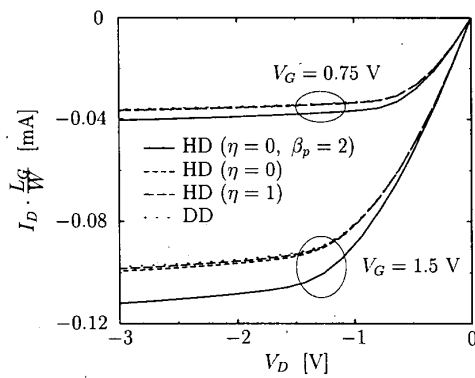Figure 4: Comparison of the output characteristics of the short-channel NMOS for both transport models.

Figure 5: Comparison of the output characteristics of the long-channel PMOS for both transport models.
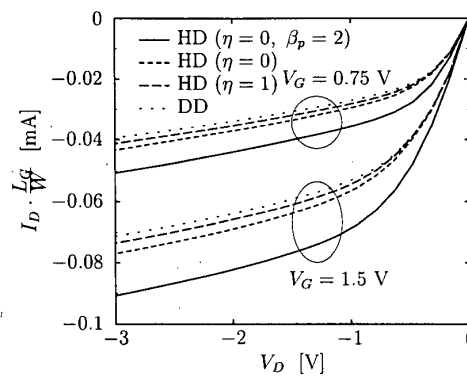

Figure 6: Comparison of the output characteristics of the short-channel PMOS for both transport models.

Monte-Carlo Method for Direct Computation of the Small Signal Kinetic Coefficients

M. Nedjalkov, H. Kosina, and S. Selberherr

Institute for Microelectronics, TU Vienna
Gusshausstr. 27–29, A-1040 Vienna, Austria

Abstract

An approach for analysis of the small signal response of the carriers in semiconductors is presented. The response to an impulse signal is explained in terms of a relaxation process, governed by a Boltzmann equation. The approach assists the understanding of the phenomenon and allows development of novel stochastic algorithms.

1. Introduction

The knowledge of the small signal response characteristics of the carriers system as depending on the frequency and the DC electric field $\mathbf{E}_s$ is of relevant importance to forecast modern device performance. Linked by the Fourier transform, analyses in the time and the frequency domains provide equivalent information. Furthermore, the response to a signal of a general time dependence $\mathbf{E}_1(t)$ can be calculated from the knowledge of the response to an impulse, $\mathbf{E}_i(t) = \delta(t)\mathbf{E}_1$. The advantages of Monte-Carlo simulations of response phenomena in the time domain have been utilized for more than two decades [1]. Within the Monte-Carlo method single-particle simulations are popular, supported by the well established theory of correlation functions of the physical characteristics over a steady state trajectory [2],[3]. Another alternative is in a transient description, given by the following derivate of the Boltzmann equation:

$$\frac{\partial f_1(\mathbf{k}, t)}{\partial t} + \frac{e}{\hbar}\mathbf{E}_s \cdot \nabla f_1(\mathbf{k}, t) = Q[f_1(\mathbf{k}, t)] - \frac{e}{\hbar}\mathbf{E}_1(t) \cdot \nabla f_s(\mathbf{k}) \tag{1}$$

$Q[f_1(\mathbf{k}, t)] = \int S(\mathbf{k}', \mathbf{k})f_1(\mathbf{k}', t)\mathrm{d}\mathbf{k} - \lambda(\mathbf{k})f_1(\mathbf{k}, t)$ is the common Boltzmann scattering term and f_1 is the correction to the distribution function f around a steady-state value f_s: $f(\mathbf{k}, t) = f_s(\mathbf{k}) + f_1(\mathbf{k}, t)$. Accordingly, the mean of a physical characteristic $A(\mathbf{k})$ is given by $\langle A \rangle(t) = \langle A \rangle_s + \langle A \rangle_1(t)$. With an impulse $\mathbf{E}_i(t)$ on the right hand side (1) cannot be treated numerically. The used stochastic or deterministic methods [2] solve (1) for the case of a step-like signal: $\mathbf{E}_{step}(t) = \theta(t)\mathbf{E}_1$. Then an impulse response characteristic $\langle A \rangle_i(t)$ is obtained by taking the time derivative of the step response $\langle A \rangle_{step}(t)$.

In this work we utilize an integral formulation of (1) for an impulse signal. It suggests a physical model of the response phenomena. The model allows to develop a new Monte-Carlo method.